Regional Environmental Change (2024) 24:173
https://doi.org/10.1007/s10113-024-02337-x

ORIGINAL ARTICLE

Woody vegetation cover on cleared areas in the Amazon Basin: temporal mixture mapping suggests a revised conceptual model of deforestation

Mallorie Honey[1] · Trent Biggs[1] · Daniel Sousa[1] · Camila Abe[1] · Katrina Mullan[2]

Received: 3 August 2023 / Accepted: 6 November 2024

Abstract

The Amazon Basin is experiencing large-scale land use conversion from primary forest to pasture. While several land cover datasets map cleared areas in the Amazon, the percent cover of woody vegetation (trees and shrubs) in cleared areas and its association with clearing age, soil type, and geology is poorly understood, despite its importance for carbon emissions, biodiversity, land–atmosphere interactions, and monitoring of pasture condition. We used temporal mixture analysis on Sentinel-2 imagery from 2019 to map woody vegetation cover on cleared areas in Rondônia, Brazil. Binary woody vegetation masks were generated at 10-m resolution using a threshold of the evergreen endmember, with an overall accuracy of 84%. The age of clearing for each pixel was calculated from MapBiomas (Sousa and Davis, Remote Sens Environ 247, 2020) with a 2019 base year. We find little evidence of large-scale abandonment of pasture: most (53%) of the cleared area in 2019 was "clean pasture" (< 10% woody vegetation cover), 34% was "dirty pasture" (10–90% woody vegetation cover), 10% was forest (90–100% woody vegetation cover), and 3% was early stage clearing (> 10% woody vegetation cover, cleared 1–5 years ago). Recently cleared areas (1–2 years) had high (60%) woody vegetation cover, woody vegetation cover decreased with pasture age, and older pastures (20–34 years) had consistently low woody vegetation cover (25% on average). The commonly observed decrease in greenness with increasing clearing age, which is sometimes interpreted as decreasing grass health, was due in part to decreasing woody vegetation cover as pastures were gradually cleared over a decade. These results suggest modifications to existing conceptual models that describe clearing as a rapid process with high rates of secondary growth. We found a gradual and semi-permanent clearing of woody vegetation and proposed a revised conceptual model of deforestation dynamics.

Keywords Deforestation · Land cover · Amazon · Remote sensing

Communicated by Wolfgang Cramer

✉ Mallorie Honey
malloriehoney@gmail.com

Trent Biggs
tbiggs@sdsu.edu

Daniel Sousa
dan.sousa@sdsu.edu

Camila Abe
cabe6547@sdsu.edu

Katrina Mullan
Katrina.Mullan@mso.umt.edu

[1] Department of Geography, San Diego State University, 5500 Campanile Dr, San Diego, CA 92182, USA

[2] Department of Economics, Montana State University, Culbertson Hall, 100, Bozeman, MT 59717, USA

Introduction

Tropical deforestation is one of the most important land use changes in the twenty-first century, with major implications for the global climate (Salati and Nobre 1991; McGuffie et al. 1995; Lawrence and Vandecar 2014), biodiversity, and economy (Barbier et al. 1991). The Amazon biome has lost approximately 20% of its primary forests since the 1960s (Assis et al. 2019), releasing carbon and potentially disrupting the regional climate (Lovejoy and Nobre 2018; Davidson et al. 2012). Pasture expansion is the leading cause of deforestation in the Amazon (Henshall 1982; Buschbacher 1986; Batistella et al. 2003; Sy et al. 2015; Veiga et al. 2002), so mapping land cover transitions on areas cleared for pasture is a key step to understanding the consequences of deforestation. In particular, the dynamics of woody vegetation, both

Published online: 02 December 2024

during and following clearing, play a key role in maintaining regional energy and carbon balances.

The transition from forest to pasture is sometimes described as relatively rapid (1–2 years) and complete, with subsequent partial abandonment and regrowth of secondary forest (Silva et al. 2020). In the Brazilian Amazon, pastures may be abandoned due to poor pasture productivity and to household lifecycles (Perz and Skole 2003; Laue and Arima 2016; Perz and Walker 2002). However, grass dominance with low woody vegetation cover can persist for decades due to either active management of productive pastures (Stahl et al. 2017) or to slow recovery of woody vegetation on infertile soils (Moran et al. 2000). The initial conversion to pasture may also not be complete; some pastures have woody scrub or shrubs, called "dirty pasture" (*pasto sujo*) (Carvalho et al. 2019), but such pastures are difficult to map. An improved understanding of woody vegetation cover dynamics is also needed to interpret time series of satellite imagery, which often show a significant decline in greenness in the first 5 years following initial clearing in the Amazon (Numata et al. 2007). While the decline in greenness with pasture age may indicate decreasing productivity of pasture grass, it may also be due to high woody vegetation (tree and shrub) cover in recently cleared areas and gradual clearing of that woody vegetation over time (Davidson et al. 2008), but the temporal patterns of woody cover in cleared areas have not been widely documented.

Several datasets map deforestation in the Amazon Basin, including MapBiomas (Souza et al. 2020) and the Brazilian Amazon Deforestation Monitoring Program (PRODES Instituto Nacional de Pesquisas Espaciais 2020), both of which use Landsat data with a spatial resolution of 30 m with a 14–16 day revisit time (Markman et al. 2004). Others have also used Landsat data and supervised classification algorithms, such as decision trees (Roberts et al. 2002) and random forest classifiers (Mu et al. 2021; Souza et al. 2020) to map land cover and rates of deforestation and secondary regrowth in the Amazon. Launched in 2015, the Sentinel 2A and 2B satellites offer improved spatial resolution (10 m) and a combined revisit time of 5 days (Drusch et al. 2012) and have been used to map forest and deforestation in the Amazon biome (Silva et al. 2022; Prudente et al. 2022).

Despite significant progress in mapping deforestation, there is little documentation of the rate of change in woody vegetation cover following clearing. Visual interpretation of high-resolution (< 1 m) aerial imagery indicates that existing land cover datasets do not sufficiently capture the heterogeneity of land cover at fine spatial scales, and many areas classified as pasture by MapBiomas have high woody vegetation density (Fig. 1). Previous work (Mu et al. 2021) mapped pastures with different woody vegetation cover, finding large areas with woody vegetation in pastures, and Carvalho et al. (2019) mapped pasture vegetation in the Brazilian state of Para in the Amazon biome based on woody

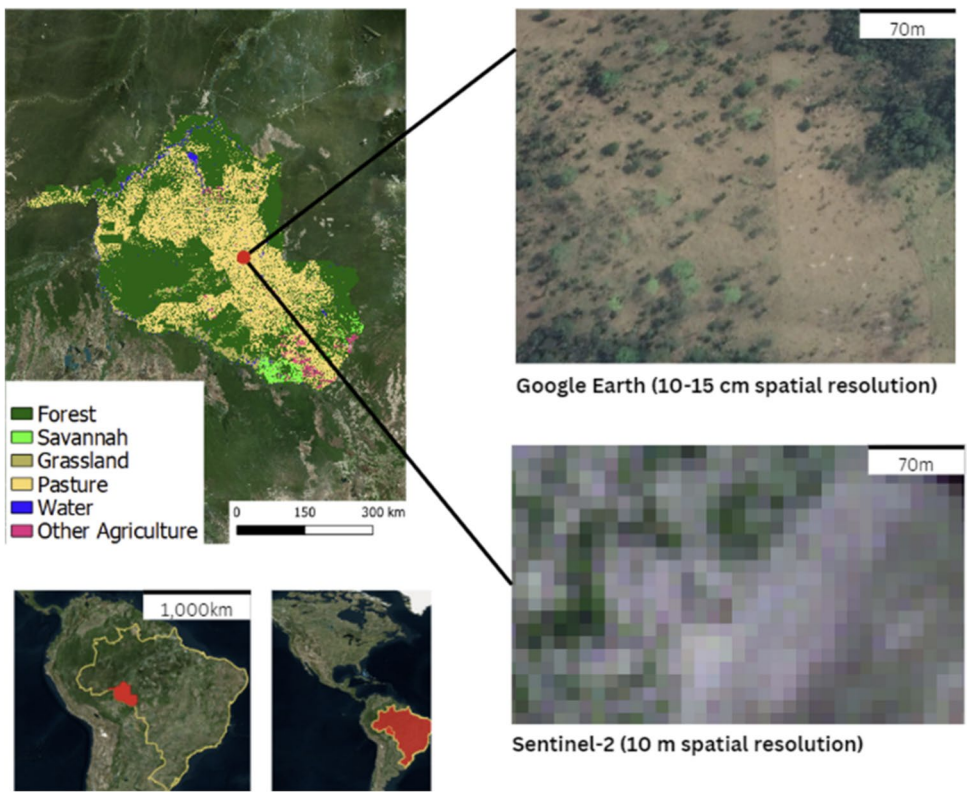

Fig. 1 Landcover in the State of Rondônia, Brazil, from the MabBiomas dataset (Souza et al. 2020) (left). Example of the heterogeneity of land cover in areas classified as "Pasture" by MapBiomas (Souza et al. 2020), from high-resolution imagery in Google Earth (top right) and 10-m resolution imagery from Sentinel-2 (bottom right)

cover, but few studies document differences in woody cover by clearing age, geology, or soil type.

Differences in seasonal phenology of grass and woody vegetation may help distinguish them in remote sensing imagery. The arc of deforestation in the southern Brazilian Amazon has a pronounced dry season from June to September, and woody vegetation often maintains greenness during the dry season longer than grasses, due to the shallow roots of grass (Davidson et al. 2012). Temporal mixture analysis uses differences in phenology to quantify the fraction of an image pixel that is covered by land cover with a given greenness pattern (Piwowar 1998; Small 2012). Temporal mixture models have been used to map dynamic surfaces like sea ice (Piwowar 1998), impervious surfaces (Yang et al. 2012), fractional tree cover (Wu et al. 2021; Sousa and Davis 2020), and crop types (Sousa and Small 2018; Zhong et al. 2015). We use temporal mixture analysis on Sentinel-2 imagery to map woody vegetation cover in the southwestern Brazilian Amazon and analyze how woody vegetation cover varies with clearing age, geology, and soil type to address the following questions:

(1) *Mapping woody vegetation cover:* How accurately can single-year temporal mixture modeling map woody vegetation cover, validated against the visual interpretation of high-resolution imagery? Does the error vary with soil type?
(2) *Spatial patterns in woody vegetation cover*: How common are "dirty" pastures with high woody vegetation cover? How does woody vegetation cover vary with clearing age?

We find that woody cover is initially high following clearing, decreases gradually for clearings between 5 and 7 years old, and is then stable with clearing age for clearings more than 10 years old. We find little evidence of widespread woody vegetation encroachment or secondary forest regeneration on old pastures. The patterns we observe contrast with some conceptual models of deforestation in the Amazon, so we propose a revised conceptual model of clearing that accommodates our observed changes in woody cover with clearing age.

Study area

The state of Rondônia (Fig. 1) is at the western end of the arc of deforestation in the Brazilian Amazon. Rondônia has experienced large-scale land use change since the 1970s, when the National Institute for Colonization and Land Reform (INCRA) began incentivizing agricultural production in the Amazon by providing zero-interest loans to small-scale farmers and investing in infrastructure and road networks (Henshall 1982; Sills and Caviglia-Harris 2009). By 2019, 34% of the forest in the state had been cleared for pasture (Souza et al. 2020). The original forest cover is a closed and open-canopy tropical forest (RADAMBRASIL 1978). Cleared areas are dominated by pasture for cattle. Soybeans are limited to the southern part of the state, and coffee and other crops are present but uncommon.

Soils in Rondônia include highly weathered Oxisols with low fertility in the north, fertile Alfisols in the central part of the state, and less fertile Ultisols and sandy Entisols in the south (Figure S4,; Cochrane and Cochrane 2006; Ballester et al. 2012). Geology includes deep clay deposits in the north, granite and gneiss in the center, metamorphosed sedimentary rocks, and sandstone in the south (Figure S9).

Methods

The methods have four components (Fig. 2): (1) woody vegetation mapping using temporal mixture analysis on a time series of Sentinel 2 imagery for 1 year (2019) ("Woody vegetation mapping"), (2) validation of the map using visual interpretation of high-resolution imagery ("Validation and evergreen thresholds"), (3) creation of land cover maps of cleared areas according to woody cover ("Land cover maps based on woody vegetation cover"), and (4) chronosequence analysis of woody vegetation cover by clearing age, soil fertility, and geology using a time series of land cover ("Chronosequence of woody vegetation cover").

Woody vegetation mapping

Data selection and preprocessing

Sentinel-2 level 2A surface reflectance images were selected, preprocessed, and downloaded for the study area using Google Earth Engine (GEE). Level 2A images have undergone atmospheric and geometric correction and identification of clouds and cloud shadows. We selected images acquired during the dry season (June–August) when woody vegetation and grass are most likely to have different greenness time series (Davidson et al. 2012).

Sentinel-2 images are organized as 110 km × 110 km tiles (Fig. 3). We selected images with low cloud cover (less than 15%) and ensured that acquisition dates were consistent among tiles. The final selection comprised 30 scenes: five dates for each of the six tiles covering June–August of 2019. Each image was cloud-masked using the "s2cloudless" algorithm available through GEE. A water mask was created of pixels with a Normalized Difference Water Index (NDWI) value greater than zero and a Normalized Difference Vegetation Index (NDVI) value less than zero. Layers of the Enhanced Vegetation Index (EVI) were mosaiced and stacked for each tile, resulting in temporal stacks with 5 bands, one for each date.

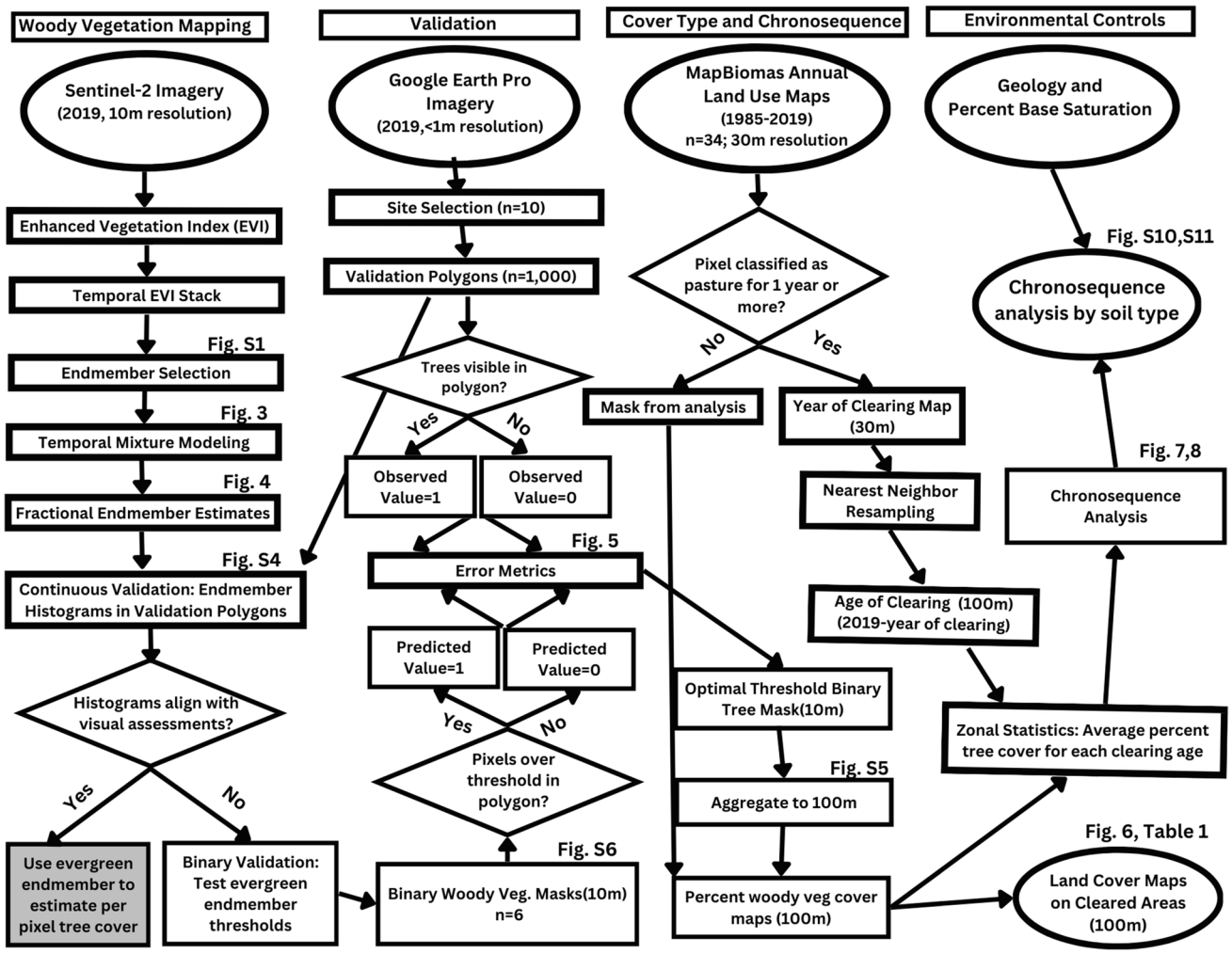

Fig. 2 Workflow diagram of data sources and methods. Workflow is split into four subsections: "Woody Vegetation Mapping," "Validation," "Cover Type and Chronosequence," and "Environmental Controls." Each subsection visualizes connections between input and output datasets (displayed in circles), processing steps (displayed in rectangles), and decision trees (displayed in diamonds with arrows pointing towards resulting processes). Additional figures are referenced throughout the flowchart near their corresponding dataset or processing step

Temporal mixture modeling

The time series of EVI for each pixel was modelled as a linear combination of temporal endmembers, each of which represents a phenological sequence such as persistent high greenness, gradually decreasing greenness, or low greenness (Piwowar 1998). Areal fractions of temporal endmembers (f_i) were estimated for each pixel using:

$$\mathrm{EV}Iobs = f_1E_1(EVI) + f_2E_2(EVI)\cdots + f_nE_n(EVI) + \varepsilon \quad (1)$$

where EVI *obs* is the observed EVI time series of a given pixel, E_i(EVI) is the time series of EVI for endmember i, and *fi* is the fractional estimate of the cover of each endmember in the given pixel (Yang et al. 2012).

Temporal endmembers of evergreen vegetation, grass, and low-EVI (E_i(EVI)) were identified from the temporal mosaic using PCA following Small (2012) (Figure S1). These endmembers were selected because they were representative of the landscape in our study zone (Fig. 4), which is comprised of rainforest fragments (evergreen vegetation), rain-fed pastures (seasonal grass), and urban areas with minimal natural vegetation (low-EVI). A fourth endmember with increasing EVI over the dry season was initially selected, but visual interpretation of Google Earth imagery suggested that this endmember did not represent a specific land cover type (Figure S2), as it highlighted small areas in both forested areas and grasslands, and included forest fragments recovering from disturbance, grass in floodplains,

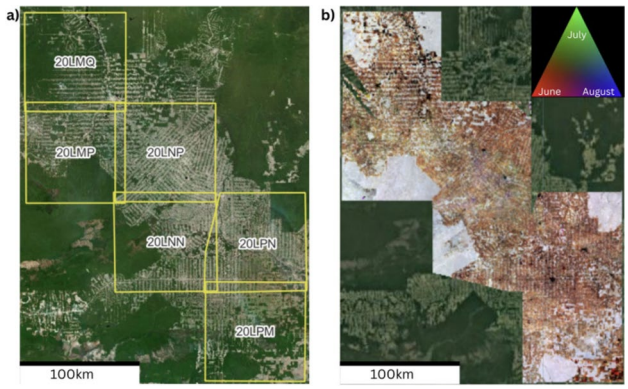

Fig. 3 **a** Map of Sentinel-2 tiling grid labeled by tiling ID. **b** RGB display of the temporal stack (right). In the temporal stack, each channel is represented by EVI values for a given date in the time series. Dates represented in (**b**) are June 10th (R), July 15th (G), and August 4th (B); white indicates high EVI in all dates, black indicates low EVI in all dates, and red indicates highest EVI in June

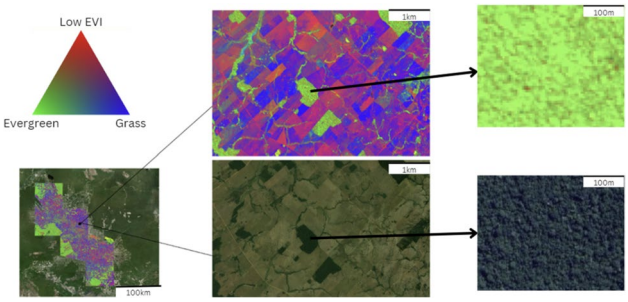

Fig. 4 Three band temporal mixture model shown in RGB color space compared with Google Earth imagery. Property boundaries and roads have high values in the low-EVI endmember band (R), and pastures are a combination of evergreen (G) and grass (B) endmembers. The close-up of a densely forested area (far right) demonstrates that forested pixels have high values in both the evergreen endmember (G) and low-EVI endmember, likely due to shade cover

or grass recovering from grazing during pasture rotation. Models with this fourth endmember underestimated woody cover (Figure S3), so the fourth endmember was omitted from the model, and the temporal mosaic was unmixed using the evergreen, grass, and low EVI endmembers.

Histograms for each of the three endmembers (evergreen, grass, low-EVI) were generated for pixels within validation polygons that had all woody vegetation cover (forest, $n=304$ polygons) or no woody vegetation cover (grass, $n=381$ polygons). Forested pixels contained a mix of "evergreen" (mean = 0.61) and "low-EVI" (mean = 0.42) endmembers, and pastures contained a mix of "evergreen" (mean = 0.2), "low-EVI" (mean = 0.48), and "grass" (mean = 0.32) endmembers (Figure S5). The low-EVI endmember in forests is mostly shade, while low-EVI in pastures is mostly bare soil. The mix of evergreen and shade endmembers in forests prevented us from interpreting the evergreen endmember fraction directly as the percent cover of woody vegetation, so we established a threshold of evergreen cover above which a pixel is labeled as "woody vegetation." We created multiple maps with evergreen thresholds ranging from 0.25 to 0.50 in increments of 0.05. For each woody vegetation map, pixels with an evergreen endmember fraction over the given threshold were classified as "Woody Vegetation" (1), and pixels falling below this threshold were classified as "No Woody Vegetation" (0).

Validation and evergreen thresholds

The woody cover maps were validated using visual interpretation of high-resolution aerial imagery available through Google Earth (GE) Pro. We selected 10 zones where 2019 GE imagery was available (Figure S8). Zones were chosen that had a range of woody vegetation cover, and zone sizes ranged from 1 to 3 km^2. Within each zone, validation points ($n=100$) were randomly generated, for a total of 1000 points. To minimize potential errors introduced by co-registration issues between high-resolution Google Earth and Sentinel-2 imagery, 30 × 30 m plots (3 × 3 Sentinel-2 pixels) were created centered on the randomly generated points. The resulting validation plots ($n=1000$) were assigned values of sparse (< 10%), partial (10–90%), and full (90–100%) woody vegetation cover using visual interpretation of the GE imagery. Due to uncertainty in estimating a specific value for woody cover fraction, we opted for categories that identified either all non-woody vegetation or some woody vegetation. In practice, most validation plots were either non-woody ($n=304$) or fully woody ($n=381$), so estimating the exact percentage of woody was not essential. The mean woody fraction for each validation plot was then calculated from the 10-m binary woody vegetation map ("Woody vegetation mapping"), and plots with any 10-m pixel over a given evergreen endmember threshold were labeled as "woody." Each validation plot was then classified as a true positive (TP), true negative (TN), false positive (FP), or false negative (FN); TS is the sum of all samples. The total error is calculated as (FP + FN)/(TS). Commission error measures the frequency of false positives as FP/(FP + TP). Omission error measures the frequency of false negatives as FN/(FN + TP).

Healthy grass that is green in the dry season might have the temporal EVI profile of woody vegetation, resulting in an overestimation of woody vegetation cover. Fertile soils may have healthier grass, so we compared the accuracy metrics of the woody cover maps for different levels of percent base saturation (PBS), which is the percent of cation exchange sites occupied by base cations (calcium, magnesium, potassium). PBS data from 3000 + soil cores were obtained from the SIGTERON project (Cochrane and Cochrane 1998) and interpolated to a 4-km resolution grid using kriging. Kriging

was implemented using the *gstat* package in R (Pebesma 2004). The variogram was calculated for each depth separately, using a spherical model. The sill, range, and nugget were determined using the *fit.variogram* function, which uses reweighted least squares and Gauss–Newton fitting. The gridded PBS map was reclassified as high (> 60%), medium (30–60%), and low (< 30%) (Figure S4, S8). The grass may also be greener in younger pastures (Numata et al. 2007), which could be confused with green woody vegetation. As our 10 initial validation zones had minimal recent land cover change, we created 5 additional zones (Figure S4) with recent deforestation (2014–2019). Accuracy metrics were summarized by PBS category for both stable cover (Table S1) and newly cleared areas (Table S2).

Land cover maps based on woody vegetation cover

The mean woody vegetation cover was calculated for areas that were classified as pasture or secondary forest in 2019 by the MapBiomas Collection 6 Dataset (Souza et al. 2020; MapBiomas 2021). The MapBiomas algorithm uses a random forest classification on Landsat imagery to assign each 30 × 30 m pixel to a land use category, such as forest, pasture, or water. The binary (0 or 1) woody vegetation layer (10-m resolution, "Woody vegetation mapping") was then aggregated to 100 m, giving a woody cover fraction for each 100-m pixel (Figure S6). Some pixels classified as "woody vegetation" at 10 m may also contain some grass and soil, so the mean woody vegetation cover is an upper-bound estimate. The classification scheme of Carvalho et al. (2019) was then modified and applied to the 100-m woody vegetation map to create a land cover map based on woody vegetation cover: clean pasture (< 10% woody vegetation), grass-dominant dirty pasture (10–50% woody vegetation), woody-dominant dirty pasture (50–90% woody vegetation), forest (90–100% woody vegetation), and early-stage clearing (> 10% woody vegetation, cleared < 5 years prior to 2019). See Figure S13 for examples of each cover type.

Chronosequence of woody vegetation cover

A space-for-time (chronosequence) (Walker et al. 2010) approach was used to analyze how woody cover varies with clearing age. The year of deforestation for each pixel was obtained from MapBiomas, which has annual land cover data for 1985–2020 at 30-m spatial resolution (Souza et al. 2020). The year of deforestation was calculated as the first year in which a pixel was classified as "Pasture" in the MapBiomas annual map collection. The age of clearing for each pixel was calculated by subtracting the year of initial deforestation from 2019. Pixels that were not classified as "Pasture" in any year (Primary Forest, Water, Urban Areas) were masked from analysis. Following Silva et al. (2020), pixels classified as "Pasture" in any previous year and "Forest" in 2019 were labeled secondary forest.

Two versions of the clearing age map were generated: one excludes secondary forests and only includes areas classified as pasture in 2019, and another includes all pixels classified as pasture during any previous year, including those classified as secondary forest in 2019. The average percent of woody vegetation cover was summarized for each clearing age using the 100-m woody vegetation map created in the "Land cover maps based on woody vegetation cover" section. To control for factors other than clearing age, a hydrogeology map from the Serviço Geológico do Brasil (*Brazilian Geological Service*) (Figure S9) was used to summarize woody cover by geology, and the PBS map created in the "Validation and evergreen thresholds" section was used to summarize woody cover by PBS (Figure S11).

Results

Temporal unmixing

The three endmembers identified from the PCA plots (evergreen, grass, and low-EVI) represented distinct land cover types (Fig. 4). Roads had high values in the low-EVI endmembers (Red in Fig. 4), while pastures have high values in both the low-EVI and grass endmembers (Blue). Forest fragments and riparian zones had high values in the evergreen endmember band (Green) interspersed with the low-EVI endmember (Red). The low-EVI endmember represented shade in forests and soil in pastures.

Validation

The 10-m woody cover map showed low overall error (16–21%). Omission and commission errors varied systemically with the evergreen fraction threshold value (Fig. 5, Figure S7): lower evergreen thresholds overestimated woody vegetation cover, while higher thresholds were underestimated. Errors of commission for the forest class included pastures near perennial water sources that stayed green through the end of the dry season (Figure S13). The evergreen endmember threshold of 0.35 was selected as the optimal threshold because it resulted in the lowest overall error (16%).

The total error of the woody vegetation cover map did not vary significantly by PBS, but errors of omission were higher on low and medium PBS, indicating a potential underestimation of woody cover on soils with low fertility (Table S1, Figure S8). The accuracy of the woody cover map was highest in newly deforested regions with high PBS (Table S2), while accuracy metrics for newly deforested validation zones with low and medium PBS levels were comparable to the

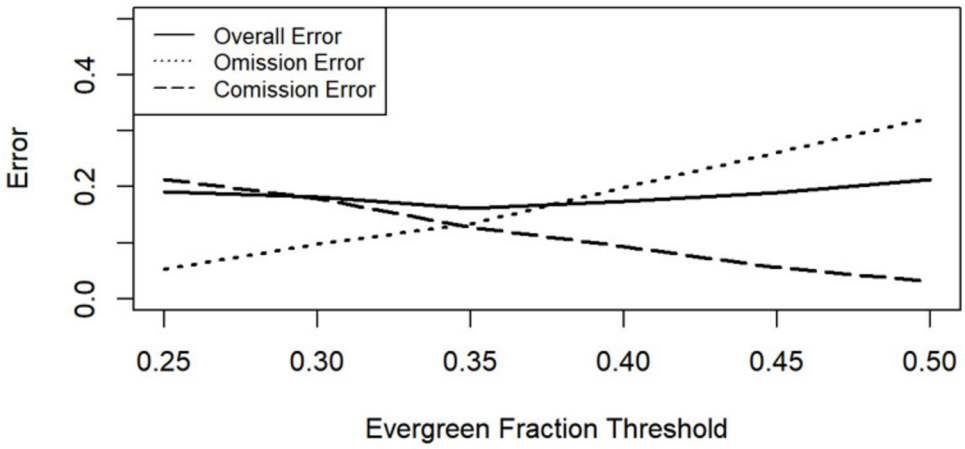

Fig. 5 Classification error of woody vegetation cover by evergreen endmember threshold value. Omission error (short-dashed line) is positively correlated with the evergreen fraction threshold value, while commission error (long-dashed line) is negatively correlated with the evergreen fraction threshold value. Overall error (solid line) is relatively consistent for a range of threshold values but is lowest at 0.35, which was selected as the optimal threshold value

study zone average. Taken together, the accuracy assessment suggests that errors were not systematically higher on more fertile soils or in newly deforested areas.

Classification of cleared areas based on woody cover

Clean pasture (< 10% woody cover) dominated (53%) the area classified as pasture or secondary forest by MapBiomas in 2019, followed by grass-dominant dirty pasture (21%), woody vegetation-dominant dirty pasture (13%), forest (10%), and early-stage clearing (3%) (Table 1). Woody-dominant pasture was most common in the center of the study region (Fig. 6). Early-stage clearing was concentrated in the northern part of the study zone, with some hotspots in the center and south. High-resolution aerial imagery (Figure S13) suggests that areas in the early stages of clearing had high woody vegetation cover but were distinct from abandoned pastures; burn scars and trails in recently cleared

Table 1 Frequency of land cover types over cleared areas

	Cover Type	Percent Area
1	Early Clearing	3.3
2	Clean Pasture	52.7
3	Dirty Pasture: Grass Dominant	21.3
4	Dirty Pasture: Woody Cover Dominant	12.5
5	Forest	10.1

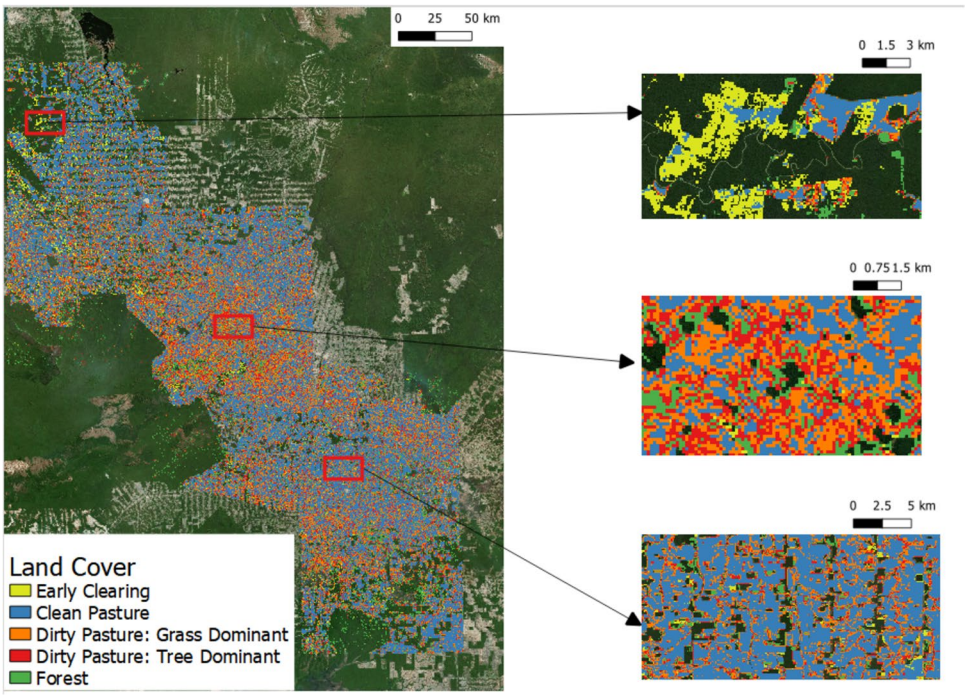

Fig. 6 Land cover types on cleared areas based on woody cover fractions displayed over a basemap of high-resolution aerial imagery. Pixels classified as primary forest by MapBiomas are omitted from the analysis

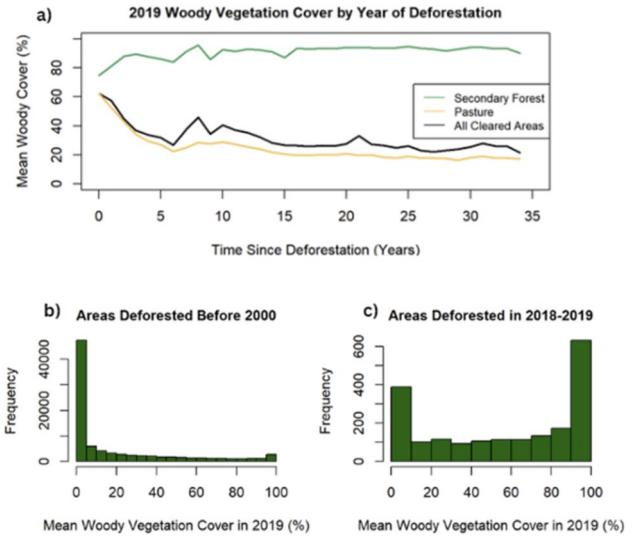

Fig. 7 Woody vegetation cover by year of deforestation for pixels classified as "Pasture" in the base year (yellow line), pixels which were classified as "Pasture" at any point between 1985 and the base-year, labeled as "All Cleared Areas" (black line), and pixels classified as "Forest" in the base-year which were classified as "Pasture" at any point prior to the base year, labeled as "Secondary Forest" (light green line) (**a**). Histograms of woody vegetation cover for the base year on areas cleared before 2000 (**b**) and between 2018 and 2019 (**c**)

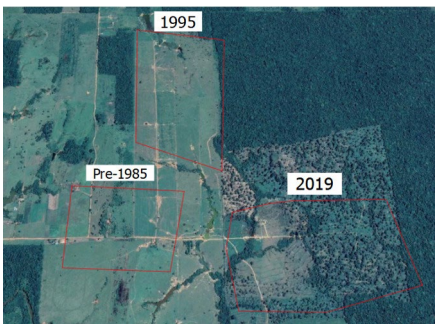

Fig. 8 Regions (delineated in red) and labeled by year of deforestation from MapBiomas overlayed on high-resolution imagery from GoogleEarth Pro. Imagery is from May 14th, 2019

areas indicated recent anthropogenic disturbance. While some areas classified as dirty pastures may be abandoned, others were adjacent to actively managed clean pastures and may be part of a rotational system. Small riparian corridors were also commonly categorized as "dirty pasture."

Chronosequence analysis

For pixels classified as either pasture or secondary forest in the MapBiomas dataset for 2019, woody vegetation cover was highest (60%) in the most recently cleared areas (1–2 years), dropped rapidly with clearing age, and was low (~25%) for clearings 20 years and older (Figs. 7a, 8). The histogram of woody cover at 100-m resolution is bimodal for areas cleared 1–2 years ago (Fig. 7c) and areas cleared 20 or more years ago (Fig. 7b), with modes at 0–5% and 95–100% cover, though half (48%) of the recently cleared area had 10–90% woody cover. Most (61%) of the 100-m pixels in the recently cleared area (1–2 years) had woody cover greater than 50% (Fig. 7c), while few (18%) had very low woody vegetation cover (less than 10%), 48% had some woody vegetation cover (10–90%), and 34% had full woody vegetation cover (90–100%). In older clearings (≥ 20 years), most (55%) of the 100-m pixels had very low woody vegetation cover, 35% had some woody vegetation cover, and 10% had full woody vegetation cover (Fig. 7b). We conclude that recently cleared areas are dominated by woody vegetation, and older clearings are dominated by non-woody cover (grass and soil).

For pixels only classified as pasture in the MapBiomas dataset for 2019, woody vegetation cover was also high on new clearings (average 58%), and low on clearings between 20 and 34 years old (average 20%). Woody vegetation cover for pastures cleared 8–10 years (30%) was also lower when secondary forests were excluded (Fig. 7a).

Just 7% of cleared areas were classified as secondary forest in the MapBiomas dataset, and the percent cover of secondary forest (MapBiomas) varied only slightly with clearing age (Figure S10). We conclude that older clearings do not have more secondary forest than recent clearings, and that woody cover is high on recently cleared areas, even after removing secondary forest from the analysis.

Effect of soil type and geology

The woody cover was similar for all soil fertility levels for older pastures (> 20 years) (Figure S11). For recently cleared (6–10 years), pastures on fertile soils had higher woody cover (51%) than the mean (42%). We conclude that woody cover remains higher for longer during clearing on fertile soils, but in the long term (> 20 years) woody cover converges to similar values for all soil types. The higher woody cover on recent clearings with fertile soils could be due to woody crops like coffee that were mapped as pasture or secondary forest by MapBiomas, to more rapid regrowth of forest on fertile soils, or to slower clearing rates on fertile soils.

The woody cover was lowest on older pastures across most geologic categories. Woody cover on pastures cleared between 6 and 10 years ago varied by geology (Figure S12): sandstone (*arenitos*) and schist (*xistos*) had the highest woody cover (67% and 58%, respectively), followed by phyllite (*filitos*) and shale (*folhelho*) (44% and 38%, respectively). Woody cover on pastures on granite and gneiss (*granitos and gnaisses*) followed a similar pattern to the study zone average. On most geologies, woody cover

for areas cleared more than 35 years was low (~25%). The only exception was sandstone (*arenitos*), which had the highest woody cover for most clearing ages. We conclude that woody cover varies by soil and geology, especially for recent clearings (< 10 years old).

Discussion

Quantifying woody cover fractions on cleared areas is important for many applications, including carbon budgets, climate models, assessments of land cover stability and sustainability, and biodiversity. We found that older pastures (deforested more than 20 years) have on average 20% woody vegetation cover, with potential implications for carbon stocks and regional climate modeling. The chronosequence analysis also suggests that existing conceptual models of deforestation require revision in our study region. In the Amazon (e.g., Silva et al. 2020; Rudel et al. 2010), the deforestation cycle has been described as a rapid process of deforestation-abandonment-regrowth, where (1) land is cleared for pasture with near-complete removal of forest vegetation using a combination of mechanical clearing and burning, (2) some of the cleared area is abandoned after several years, and (3) slowly replaced by secondary forest and shrubland or dirty pasture (Fig. 9). Our results suggest that deforestation is instead a gradual, multiyear to decadal process in which stands of contiguous forest are only partially cleared and disturbed, then gradually cleared by rows or sections (Figs. 7, 8, 9). In the gradual clearing model, woody cover declines monotonically with clearing age, and older pastures have relatively low woody vegetation cover, indicating complete clearing rather than abandonment. This finding agrees with Rufin et al. (2015) who document increased land use intensity and less woody cover in older pastures compared with recent clearings. The low woody cover on pastures in Rondônia may be related to lower primary deforestation rates in the "old frontier" (Caviglia-Harris et al. 2015), which increases pressure on existing cleared areas and encourages their re-conversion to clean pasture (Carvalho et al. 2019). The effect of socioeconomic and policy pressures on woody vegetation dynamics requires further investigation.

The deforestation-abandonment-regrowth model assumes that pastures are abandoned after several years due to declining productivity, indicating a negative feedback loop in which farmers lose the incentive to cultivate the land, allowing the natural landscape to recover. Our results indicate that clearing increases over time to near completion, with little land abandonment and regrowth.

The temporal pattern in woody vegetation also has implications for monitoring the health and productivity of pasture grass. The gradual decline in woody vegetation cover on newly cleared pastures coincides with an apparent decline in pasture health after 5–10 years found in previous studies (Numata et al. 2007). Based on our results, the drop in green vegetation on new pastures is likely caused by the clearing of woody vegetation, rather than the degradation of grass

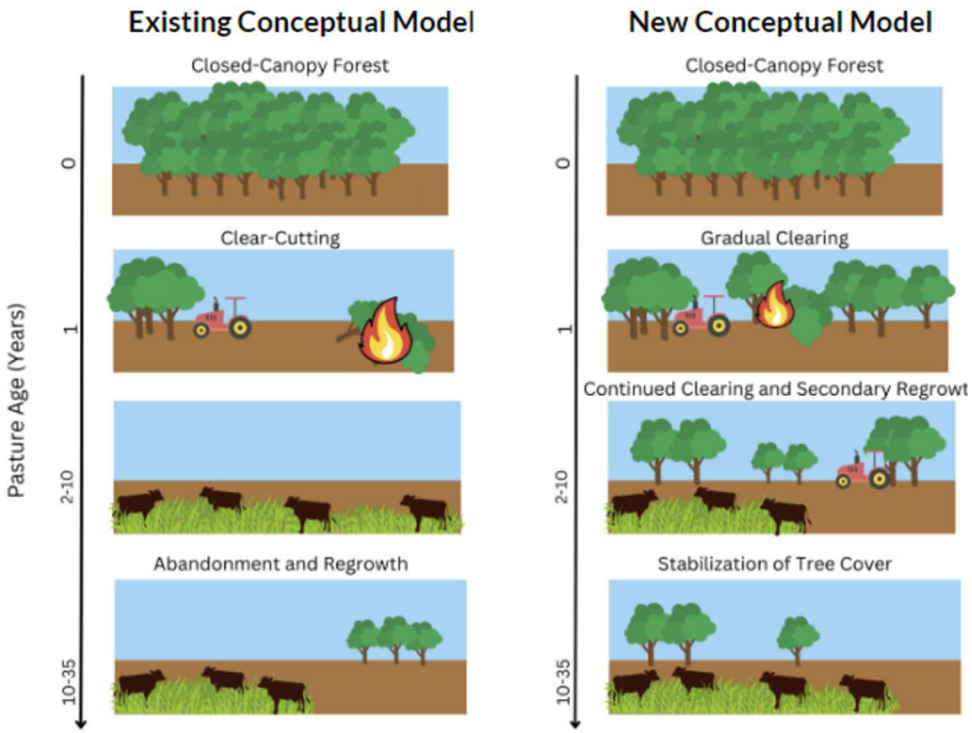

Fig. 9 Existing conceptual model of deforestation showing clear-cutting and regrowth (Silva et al. 2022) (left) and proposed conceptual model showing gradual clearing and stabilization of woody vegetation cover (right)

quality or condition, as noted by Davidson et al. (2008), although further research is needed to understand the impact of woody vegetation on pasture health estimates.

Limitations

We used a chronosequence (space-for-time substitution) to analyze temporal patterns of woody vegetation cover on pastures and tested for the impact of soil fertility (percent base saturation) and geology on woody cover, in part because it was difficult to find cloud-free imagery of the same dates for multiple years. Our chronosequence analysis therefore does not illustrate how woody cover changes over time at a given location, but rather how woody cover varies over space, with clearing age as a major explanatory variable. Spatial variations in woody cover may also be influenced by factors other than clearing age that were not analyzed here, such as variations in policies or enforcement, demographics, history of settlement and clearing, topography, and infrastructure development such as road construction and paving.

The MapBiomas dataset was used to calculate the age of clearing and to document temporal patterns of secondary forest regrowth. While the MapBiomas dataset has relatively high accuracy (91%), our results may be influenced by errors in this dataset. In particular, transitions from forest to pasture and pasture to secondary forest may be due to changes in spectral properties unrelated to changes in land cover, leading to errors in estimating clearing age. Additionally, the integration of datasets with different spatial resolutions may influence accuracy. The percent woody cover map at 100 m was aggregated from 10-m binary woody cover maps. Some 10-m pixels classified as "woody vegetation" also contained some bare soil and grass, so the percent woody cover is likely an upper-bound estimate. The year of deforestation layer derived from MapBiomas was aggregated to 100 m using nearest neighbor resampling, which relies on the assumption that adjacent pixels will have similar values. This assumption is likely not true for all pixels in our study zone, especially along the boundaries of old and new clearings, leading to potential errors in clearing ages. The soil fertility layer (PBS) had a 4 km resolution and the geology map had a scale of 1:1,000,000, which is significantly coarser than the 10-m woody cover map, though we assume here that soil fertility is highly spatially autocorrelated and can be estimated well from coarse resolution maps. Finally, our maps of pasture condition based on woody cover (Fig. 6) is highly scale-dependent; at fine resolution (10 m) most pixels are either all woody vegetation or all grass due to the canopy and stand size of woody vegetation; at coarser resolution (1 km) the histogram of woody cover would likely become less bimodal, resulting in less "pure" cover types (all grass, all woody) and more mixed pasture types. More work is needed to determine the spatial resolution that farmers use to classify and manage their land and to better understand how given classes result from management decisions and how the farmer's understanding of pasture condition and woody cover translates into management decisions such as fallowing or abandonment or use of fire for clearing.

In the absence of ground observations of land cover, we used visual interpretation of high-resolution imagery, similar to other studies, to validate land use maps generated from lower-resolution satellite imagery (Roberts et al. 2002). While we are confident that woody cover could be identified with visual interpretation, additional ground data on woody cover fraction and species composition would assist with image interpretation. Additionally, spaceborne light detection and ranging (LiDAR) datasets have been used in more recent studies to validate vegetation mapping from multispectral satellites (Milenkovic et al. 2022) by comparing elevation estimates from LiDAR data to verify that land cover maps can discriminate between classes with similar spectral signatures, such as trees and green grass, and could increase both the accuracy and interpretation of the woody cover maps generated here.

Some riparian grasslands were mapped as woody vegetation because evergreen woody vegetation has a similar temporal profile to riparian grasslands that maintain high EVI through the dry season. Therefore, some healthy pastures were miscategorized as early-stage clearing or secondary forest in Fig. 6. This issue could be mitigated by including additional satellite imagery such as Sentinel-1, which uses synthetic aperture radar (SAR), and GEDI (Di Tommaso et al. 2024), which uses LiDAR, into a rule-based classification system.

Conclusion

We used temporal mixture modeling on Sentinel-2 imagery to map woody vegetation in deforested areas of the southwestern Amazon. A binary thresholding approach yielded high overall accuracy (84%). A chronosequence (space-for-time) approach documented that (1) woody cover was high from the year of clearing up to 5–10 years, and woody cover gradually decreased between 1 and 10 years and was low and similar for all clearings more than 10 years old; (2) large-scale land abandonment or reversion to "dirty pasture" or secondary forest was uncommon; and (3) woody cover was higher on fertile than on infertile soils for clearings 8–10 years old but was similar across all soil types for clearings older than 15–20 years. Our results suggest a revision to conceptual models of deforestation, with high woody cover during initial clearing phases and low but stable woody cover for older clearings, resulting in permanent grasslands with stable cover for decades following clearing.

Deforestation in our study region, then, was a gradual and permanent process with stable long-term cover rather than a rapid and temporary one with high rates of woody cover regrowth. This model may not hold in other regions of the Amazon with different soil, socioeconomic, or policy contexts, and more work is needed to determine which model (clear-abandon-regrowth or gradual-complete-stable) applies in different contexts.

Supplementary Information The online version contains supplementary material available at https://doi.org/10.1007/s10113-024-02337-x.

Acknowledgements The Age of Deforestation layer was generated from Google Earth Engine codes written by Kyle Jones, San Diego State University. Funding for this study was provided in part by the National Science Foundation (CNH-L award 1825046) and a graduate assistantship from San Diego State University. Daniel Sousa gratefully acknowledge funding from NASA EMIT Science and Applications Team Program (Grant #80NSSC24K0861), the USDA NIFA Sustainable Agroecosystems program (Grant #2022-67019-36397), the USDA AFRI Rapid Response to Extreme Weather Events Across Food and Agricultural Systems program (Grant #2023-68016-40683), the NASA Land-Cover/Land Use Change program (Grant #NNH21ZDA001N-LCLUC), the NASA Remote Sensing of Water Quality program (Grant #80NSSC22K0907), the NASA Applications-Oriented Augmentations for Research and Analysis Program (Grant #80NSSC23K1460), the NASA Commercial Smallsat Data Analysis Program (Grant #80NSSC24K0052), the NASA FireSense Implementation Team (Grant #80NSSC24K1320) and airborne science program (Grant #80NSSC24K0145), the California Climate Action Seed Award Program, and the NSF Signals in the Soil program (Award #2226649).

References

Assis LFFG, Ferreira KR, Vinhas L, Maurano L, Almeida C et al (2019) TerraBrasilis: a spatial data analytics infrastructure for large-scale thematic mapping. Int j Geo-Inform 8:513. https://doi.org/10.3390/ijgi8110513

Ballester MVR, Victoria DC, Krusche AV, Victoria RL, Richey JE (2012) LBA-ECO CD-06 Soil Classification Map, Ji-Parana River Basin, Rondonia, Brazil. Data set. Available on-line [http://daac.ornl.gov] from Oak Ridge National Laboratory Distributed Active Archive Center, Oak Ridge, Tennessee, USA. https://doi.org/10.3334/ORNLDAAC/1088

Barbier EB, Burgess JC, Markandya A (1991) The economics of tropical deforestation. Land Econ 20:55–58. https://doi.org/10.2307/3147087

Batistella M, Robeson SM, Moran E (2003) Settlement design, forest fragmentation, and landscape change in Rondônia, Amazônia. Photogramm Eng Remote Sens 69:805–812. https://doi.org/10.14358/PERS.69.7.805

Buschbacher R (1986) Tropical deforestation and pasture development. Bioscience 36(1):22–28. https://doi.org/10.2307/1309794

Carvalho R, Adami M, Amaral S, Bezerra FG, de Aguiar APD (2019) Changes in secondary vegetation dynamics in a context of decreasing deforestation rates in Pará, Brazilian Amazon. Appl Geogr 106:40–49. https://doi.org/10.1016/j.apgeog.2019.03.001

Caviglia-Harris JL, Toomey M, Harris DW, Mullan K, Bell AR et al (2015) Detecting and interpreting secondary forest on an old Amazonian frontier. J Land Use Sci 10(4):442–565. https://doi.org/10.1080/1747423X.2014.940614

Cochrane TT, Cochrane TA (1998) Sigteron: Sistema de Informação geográfica para os terrenos e solos do estado de Rondônia, Brasil. Porto Velho: Tecnosolo/DHV Consultants BV

Cochrane TT, Cochrane TA (2006) Diversity of the land resources in the Amazonian State of Rondônia, Brazil. Acta Amazon 36:91–102. https://doi.org/10.1590/S0044-59672006000100011

Davidson EA, Asner GP, Stone TA, Neill C, Figueiredo RO (2008) Objective indicators of pasture degradation from spectral mixture analysis of Landsat imagery. J Geophys Res 113(G1):G00B3. https://doi.org/10.1029/2007JG000622

Davidson EA, De Araújo AC, Artaxo P, Balch JK, Brown IF et al (2012) The Amazon Basin in transition. Nature 481:321–328. https://doi.org/10.1038/nature10717

Di Tommaso S, Wang S, Strey R, Lobell DB (2024) Mapping sugarcane globally at 10 m resolution using GEDI and Sentinel-2. Earth Syst Sci Data 16(10):4931–4947. https://doi.org/10.5194/essd-16-4931-2024

Drusch M, Del Bello U, Carlier S, Colin O, Fernandez V et al (2012) Sentinel-2: ESA's optical high-resolution mission for GMES operational services. Remote Sens Environ 120:25–36. https://doi.org/10.1016/j.rse.2011.11.026

Henshall JD (1982) Agricultural colonization in Rondônia, Brazil. Luso-Braz Rev 19:169–185

Instituto Nacional de Pesquisas Espaciais (INPE) (2020) Portal TerraBrasilis. http://terrabrasilis.dpi.inpe.br.

Laue JE, Arima EY (2016) Spatially explicit models of land abandonment in the Amazon. J Land Use Sci 11:48–75. https://doi.org/10.1080/1747423X.2014.993341

Lawrence D, Vandecar K (2014) Effects of tropical deforestation on climate and agriculture. Nat Clim Chang 5:27–36. https://doi.org/10.1038/nclimate2430

Lovejoy TE, Nobre C (2018) Amazon tipping point. Sci Adv 4:eaat2340. https://doi.org/10.1126/sciadv.aat2340

MapBiomas (2021) Collection 6 of the annual series of land use and land cover maps of Brazil. https://mapbiomas.org/download, access date June 10, 2024

Markman BL, Storey JC, Williams DL, Irons JR (2004) Landsat sensor performance: history and current status. IEEE Trans Geosci Remote Sens 42(12):2691–2694. https://doi.org/10.1109/TGRS.2004.840720

McGuffie K, Henderson-Sellers A, Zang H, Durbidge TB, Pitman AJ (1995) Global climate sensitivity to tropical deforestation. Global Planet Change 10(1–4):97–128. https://doi.org/10.1016/0921-8181(94)00022-6

Milenković M, Reiche J, Armston J, Neuenschwander A, De Keersmaecker W et al (2022) Assessing amazon rainforest regrowth with GEDI and ICESat-2 data. Sci Remote Sens 5:100051. https://doi.org/10.1016/j.srs.2022.100051

Moran EF, Brondizio ES, Tucker JM, Da Silva-Forsberg MC, McCracken S et al (2000) Effects of soil fertility and land-use on forest succession in Amazônia. For Ecol Manage 139:93–108. https://doi.org/10.1016/S0378-1127(99)00337-0

Mu Y, Biggs TW, De Sales F (2021) Forests mitigate drought in an agricultural region of the Brazilian Amazon: atmospheric moisture tracking to identify critical source areas. Geophys Res Lett 41:8682–8692. https://doi.org/10.1029/2020GL091380

Numata I, Roberts DA, Sawada Y, Chadwick OA, Schimel JP et al (2007) Regional characterization of pasture changes through time and space in Rondonia, Brazil. Earth Interact 11:1–25. https://doi.org/10.1175/EI232.1

Pebesma EJ (2004) Multivariable geostatistics in S: the gstat package. Comput Geosci 30:683–691. https://doi.org/10.1016/j.cageo.2004.03.012

Perz SG, Skole DL (2003) Secondary forest expansion in the Brazilian Amazon and the refinement of forest transition theory. Soc Nat Resour 16:277–294. https://doi.org/10.1080/08941920390178856

Perz SG, Walker RT (2002) Household life cycles and secondary forest cover among small farm colonists in the Amazon. World Dev 30:1009–1027. https://doi.org/10.1016/S0305-750X(02)00024-4

Piwowar J (1998) Temporal mixture analysis of arctic sea ice imagery: a new approach for monitoring environmental change. Int J Appl Earth Obs Geoinf 10:92–108. https://doi.org/10.1016/j.jag.2007.10.001

Prudente VHR, Skakun S, Oldoni LV, Haron AM, Maristela R et al (2022) Multisensor approach to land use and land cover mapping in Brazilian Amazon. ISPRS J Photogramm Remote Sens 189:95–109. https://doi.org/10.1016/j.isprsjprs.2022.04.025

RADAMBRASIL (1978) Levantamento de recursos naturais. Ministerio das Minas e Energia, Rio de Janeiro, Brazil

Roberts DA, Numata I, Holmes K, Batista G, Krug T et al (2002) Large area mapping of land-cover change in Rondônia using multitemporal spectral mixture analysis and decision tree classifiers. J Geophys Res 107(D20):8073. https://doi.org/10.1029/2001JD000374

Rudel TK, Schneider L, Uriarte M (2010) Forest transitions: an introduction. Land Use Policy 27:95–97. https://doi.org/10.1016/j.landusepol.2009.09.021

Rufin P, Müller H, Pflugmacher D, Hostert P (2015) Land use intensity trajectories on Amazonian pastures derived from Landsat time series. Int J Appl Earth Obs Geoinf 41:1–10. https://doi.org/10.1016/j.jag.2015.04.010

Salati E, Nobre CA (1991) Possible climatic impacts of tropical deforestation. Clim Change 19:177–196. https://doi.org/10.1007/BF00142225

Sills E, Caviglia-Harris JL (2009) Evolution of the Amazonian frontier: land values in Rondônia, Brazil. Land Use Policy 26:55–67. https://doi.org/10.1016/j.landusepol.2007.12.002

Silva CA, Guerrisi G, Del Frate F, Sano EE (2022) Near-real time deforestation detection in the Brazilian Amazon with Sentinel-1 and neural networks. Eur J Remote Sens 55:129–149. https://doi.org/10.1080/22797254.2021.2025154

Silva Junior CHL, Heinrich VHA, Freire ATG, Broggio IS, Rosan TM et al (2020) Benchmark maps of 33 years of secondary forest age for Brazil. Sci Data 7:269. https://doi.org/10.1038/s41597-020-00600-4

Small C (2012) Spatiotemporal dimensionality and time-space characterization of multitemporal imagery. Remote Sens Environ 124:793–809. https://doi.org/10.1016/j.rse.2012.05.031

Sousa D, Davis F (2020) Scalable mapping and monitoring of Mediterranean-climate oak landscapes with temporal mixture models. Remote Sens Environ 247:111937. https://doi.org/10.1016/j.rse.2020.111937

Sousa D, Small C (2018) Mapping and monitoring rice agriculture with multisensor temporal mixture models. Remote Sens 11(2):181. https://doi.org/10.3390/rs11020181

Souza CM, Shimbo JZ, Rosa MR, Parente LL, Alencar AA et al (2020) Reconstructing three decades of land use and land cover changes in Brazilian biomes with Landsat archive and earth engine. Remote Sens 12:2735. https://doi.org/10.3390/rs12172735

Stahl C, Fontaine S, Klumpp K, Picon-Cochard C, Grise MM et al (2017) Continuous soil carbon storage of old permanent pastures in Amazonia. Glob Change Biol 23:3382–3392. https://doi.org/10.1111/gcb.13573

Sy VD, Herold M, Achard F, Beuchle R, Clevers JGPW et al (2015) Land use patterns and related carbon losses following deforestation in South America. Environ Res Lett 10:124004. https://doi.org/10.1088/1748-9326/10/12/124004

Veiga JB, Tourrand JF, Poccard-Chapuis R, Piketty MG (2002) Cattle ranching in the Amazon rainforest. Anim Prod 24:253–256

Walker LR, Wardle DA, Bardgett RD, Clarkson BD (2010) The use of chronosequences in studies of ecological succession and soil development. J Ecol 98:725–736. https://doi.org/10.1111/j.1365-2745.2010.01664.x

Wu T, Zhao Y, Wang S, Su H, Yang Y et al (2021) Improving the accuracy of fractional evergreen forest cover estimation at subpixel scale in cloudy and rainy areas by harmonizing Landsat-8 and Sentinel-2 time-series data. IEEE J Sel Topics Appl Earth Observ Remote Sens 14:3373–3385. https://doi.org/10.1109/JSTARS.2021.3064580

Yang F, Matsushita B, Fukushima T, Yang W (2012) Temporal mixture analysis for estimating impervious surface area from multi-temporal MODIS NDVI data in Japan. ISPRS J Photogramm Remote Sens 70:90–98. https://doi.org/10.1016/j.isprsjprs.2012.05.016

Zhong C, Wang C, Wu C (2015) MODIS-based fractional crop mapping in the U.S. Midwest with spatially constrained phenological mixture analysis. Remote Sens 7:512–529. https://doi.org/10.3390/rs70100512